Cerebral Cortex February 2005;15:152-165
doi:10.1093/cercor/bhh118
Advance Access publication July 6, 2004

Axons in Cat Visual Cortex are Topologically Self-similar

Tom Binzegger[1,2], Rodney J. Douglas[1] and Kevan A.C. Martin[1]

[1]Institute of Neuroinformatics, University of Zürich and ETH Zürich, Winterthurerstrasse 190, 8057 Zürich, Switzerland and [2]Henry Wellcome Building for Neuroecology, University of Newcastle upon Tyne NE2 4HH, UK

The axonal arbors of the different types of neocortical and thalamic neurons appear highly dissimilar when viewed in conventional 2D reconstructions. Nevertheless, we have found that their one-dimensional metrics and topologies are surprisingly similar. To discover this, we analysed the axonal branching pattern of 39 neurons (23 spiny, 13 smooth and three thalamic axons) that were filled intracellularly with horseradish peroxidase (HRP) during *in vivo* experiments in cat area 17. The axons were completely reconstructed and translated into dendrograms. Topological, fractal and Horton–Strahler analyses indicated that axons of smooth and spiny neurons had similar complexity, length ratios (a measure of the relative increase in the length of collateral segments as the axon branches) and bifurcation ratios (a measure of the relative increase in the number of collateral segments as the axon branches). We show that a simple random branching model (Galton–Watson process) predicts with reasonable accuracy the bifurcation ratio, length ratio and collateral length distribution of the axonal arbors.

Keywords: cell types, dendrogram, 3D reconstruction, fractal analysis, Galton–Watson branching process, Horton–Strahler method

Introduction

The overall gestalt of a neuron, usually viewed in two dimensions, has had a powerful influence on ideas of how cortical circuits are organized and function (Lorente de Nó, 1949; Jones, 1975; Lund and Boothe, 1975; Szentagothai, 1975; Lund *et al.*, 1979). It is only in recent years that it has become possible to quantify the gestalt by direct measurements. Until now, however, quantitative analyses of neuronal morphology have focused almost entirely on the dendritic tree (Uylings and Van Pelt, 2002). The axon morphology has been much harder to demonstrate and analyze and so there has been comparative neglect of axon structure. Cortical anatomists have largely provided qualitative or generic descriptions of axon morphologies (Ramón y Cajal, 1908), or have documented the morphology of individual axons labeled with bulk methods (Rockland, 1995). These anatomical studies have been essential steps in piecing together the puzzle of the cortical circuits and have prompted theoretical investigations as to how simple rules such as the conservation of 'wire' may lead to the observed maps (Mitchison and Crick, 1982; Koulakov and Chklovskii, 2001). Axon metrics, such as the average axon length, have been estimated from electron microscopic data (Foh *et al.*, 1973; Braitenberg and Schüz, 1991), supported by occasional measurements made on single cells filled with tracers *in vivo* (Kisvárday *et al.*, 1985, 1986; Tettoni *et al.*, 1998) or *in vitro* (Gupta *et al.*, 2000). Topological analyses (i.e. the analysis of the connectional or 'logical' arrangement of the branches in a tree, rather than the spatial pattern formed in the three dimensional space) have been made for axons in the frog (Bart *et al.*, 2000) and fish (Triller and Korn, 1986). Innocenti and colleagues made a topological analysis of cortical axons that project long distances, i.e. callosal axons in the cat and thalamic axons in the mouse and explored how the geometry of axons relates to their computation properties (Innocenti *et al.*, 1994; Tettoni *et al.*, 1998).

Nearly absent from the literature are metrical or topological comparisons of the axonal arborizations of different cortical neurons within the same cortical area. While it is clear that axons of different neural types have different laminar preferences and different lateral extents, what we do not know is whether these differences are simply variations on a theme, like different breeds of horses or dogs, or whether they reflect fundamentally different 'species', each with its own rule of pattern formation. By analogy, simply measuring the dimensions of axons will not reveal whether they have structural properties in common. In this paper we compare structures of the axons of different neurons drawn from a single cortical area, with the aim of establishing the similarities and differences in the structure of different axons, beyond the obvious differences of their patterns of laminar innervation and horizontal spread. We therefore include in our analyses metrical parameters, e.g. the collateral length, and topological parameters, which are sensitive only to the number and structural arrangement of the collaterals within the tree, e.g. the number of segments between origin and tip. Analyses of parameters that rely on the 3D shape of the axonal tree, e.g. the branch angles and branch locations in the neuropil, are beyond the scope of the present work.

Establishing whether there are relationships between the different types will contribute to current debates of diversity versus stereotypy of cortical neurons. These issues are important, because they address implicitly a deep problem: how do cortical neuronal circuits assemble themselves using a relatively small amount of genetic instruction? Here we discovered that axons of different neurons share more topological and metrical properties than are immediately apparent from their traditional 2D gestalts.

Material and Methods

Preparations and Maintenance of Animals

The axons examined in this study were obtained from anaesthetized adult cats that had been prepared for *in vivo* intracellular recording (for details, see Martin and Whitteridge, 1984; Douglas *et al.*, 1991). The same set of axons was also used in another study (Anderson *et al.*, 2002). All experiments were carried out by Kevan Martin and colleagues under the authorization of animal research licenses granted by the Home Office of the UK and the Cantonal Veterinary Authority of Zürich. We first recorded from each cell extracellularly and mapped the receptive field orientation preference, size, type, binocularity and direction

preference by hand. The mapping was repeated intracellularly and horseradish peroxidase (HRP) was then ionophoresed into the cell. Thalamic afferents were classified as X- or Y-type using a battery of tests (Friedlander and Stanford, 1984; Martin and Whitteridge, 1984). After appropriate survival times, the brains were fixed, sectioned at 80 μm with a Vibratome and processed to reveal the HRP and then osmicated and embedded in resin to eliminate differential shrinkage. The reconstructions were done in 3D so that the correct lengths of axons could be accurately measured. Our estimate of the shrinkage of the tissue is 11%. This is far lower than is usual in material prepared for light microscopy with the more common method of air-drying, which on our estimate results in a shrinkage of 80% in the thickness of the section and less severe, but variable amounts in the X- and Y-dimensions. The lengths given in the dendrograms are the Euclidean lengths estimated from the 3D coordinates of the axon and are corrected for the shrinkage.

Cell Reconstructions

Neurons were reconstructed in three dimensions at ×400 magnification with the aid of a light microscope (Leitz Dialux 22) with drawing tube attached to an in-house 3D reconstruction system (TRAKA). TRAKA was written in PASCAL by Rodney Douglas and Danie Botha. The reconstructions were characterized by a list of data points consisting of a code describing the digitized structure (axon, bouton or dendrite) and its three spatial co-ordinates and thickness (where relevant). The somata of the neurons each gave rise to only one axon. The axonal arborizations were complex and often extended through many histological sections. The pieces in each section were merged to form a single tree. Occasionally labeled collaterals could not be connected: these were ignored in the analysis. The measurement error of the digitized structures was estimated by measuring four boutons ten times. The standard deviation was smaller than 0.6 μm in all three dimensions. The data were rotated in order to bring all reconstructed cells into the same coordinate system.

Metrical and Topological Analysis

Axonal trees are complex structures and it is impossible to provide a single compact and coherent description of all their attributes. Here we focus on collateral length, collateral frequency and the arrangement of these collaterals within the tree. This information is contained within the 3D tree, but it is much more conveniently represented by the simpler 2D binary tree, called the 'dendrogram'. (In the present context the word 'axogram' would seem more appropriate, but we defer to the generic technical term derived from Greek for 'tree'). A dendrogram is simply a flattened version of the three dimensional axonal tree, in which the polygons representing the axon collaterals are stretched out and arranged so that the collaterals do not intersect (Figs 1–3). The dendrogram is the appropriate representation to use here, because it is independent of the actual three-dimensional embedding of the axonal tree in the neuropil. In the process of making the dendrogram, the relationships between the different collaterals were carefully maintained. If two collaterals in the axonal tree branched from the same mother collateral, then the same two collaterals also branch from the same mother collateral in the dendrogram.

We investigated metrical key features of the global properties of the dendrogram using a histogram of the collateral lengths. Various measures that describe the topology of the axonal trees, e.g. the number of collateral segments between the root and a terminal collateral, are defined in the nomenclature of topology below. These simple measures provide a first level quantitative description that enable different axons to be compared directly. To relate different sets of collaterals within the axonal tree to each other, we used the Horton–Strahler method, which introduces generations of branches: the first generation are the outermost branches, and the last generation of branches contains the root of the tree. This allows the change in length and frequency of branches between consecutive generations to be compared and the 'growth' rules of the tree to be inferred.

Magnitude, Depth, Height and Exterior Path Length

An axonal tree, or its representation as a dendrogram (Figs 2 and 3), is a binary tree consisting of three types of collaterals. The 'root collateral' connects the origin of the tree (i.e. the cell body) with the first branch point, the 'end collaterals' are the collaterals that have no children and thus terminate the branching, and the 'inner collaterals' are all collaterals which are not end-collaterals (i.e. the root collateral is also an inner collateral).

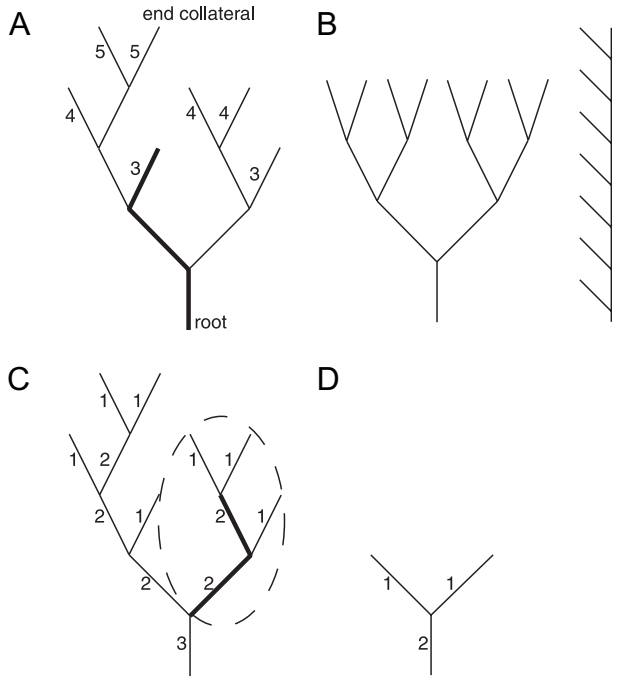

Figure 1. Parameters used to describe the topology of binary trees. (*A*) The number of end collaterals is the 'magnitude' of the tree. Any given end collateral has a 'depth' value, which indicates the minimal number of collaterals in a path that connects the root and the end collateral. One such path with three collaterals is indicated with a bold line. The 'height' of the tree is the maximum depth occurring in the tree: in this example it is 5. The 'exterior path length' is the sum of depths of the end collaterals, in this example it is 28. (*B*) 'Dichotomous' tree (left) and 'herringbone' tree (right) of magnitude $\nu_0 = 8$. (*C*) Each number indicates the 'Horton–Strahler order' of a collateral. By definition each end collateral has order 1. Collaterals with children of similar order k have order $k + 1$. Collaterals with children of different orders k_1 and k_2 have order $\max(k_1, k_2)$. A 'segment' of order k is a maximum chain of collaterals of this order. A segment of order 2 is indicated with a bold line. A 'subtree of order 2' is enclosed by the stippled line. The 'Strahler number' is the highest order in the tree, here it is 3. (*D*) Binary tree that results when the tree shown in *C* was pruned. This operation cuts all end collaterals and the collaterals of the new tree are ordered again. The segments of order 2 of the old tree become the end collaterals of the pruned tree.

The 'magnitude' (ν_0) of a tree is defined as the number of end collaterals it contains, and is related to the total number of collaterals (ν_1) in the tree by $\nu_1 = 2\nu_0 - 1$. (It follows that the number of inner collaterals equals the number of end collaterals minus 1.)

The 'depth' of a particular end collateral is the number of collaterals (including the root collateral and the end collateral itself) along the shortest path between the root and the particular termination (Fig. 1*A*). The 'height' is the maximum depth of all the end collaterals. The 'exterior path length' is the sum of the depths of all the end collaterals.

It is easy to see that both the height and the exterior path length are not independent of the magnitude of the tree. A large exterior path length can be achieved if there are a large number of end collaterals (i.e. the magnitude of the tree is large) or if the end collaterals have a large depth. With increasing magnitude, the height will tend to increase too. Thus, direct comparison of the height or exterior path length is of little significance for trees with very different magnitudes. We therefore plotted these two parameters as a function of magnitude.

Tree Asymmetry Index

Pelt *et al.* (1992) proposed a topological index that measures the asymmetry of a binary tree. The definition is based on the partition asymmetry index

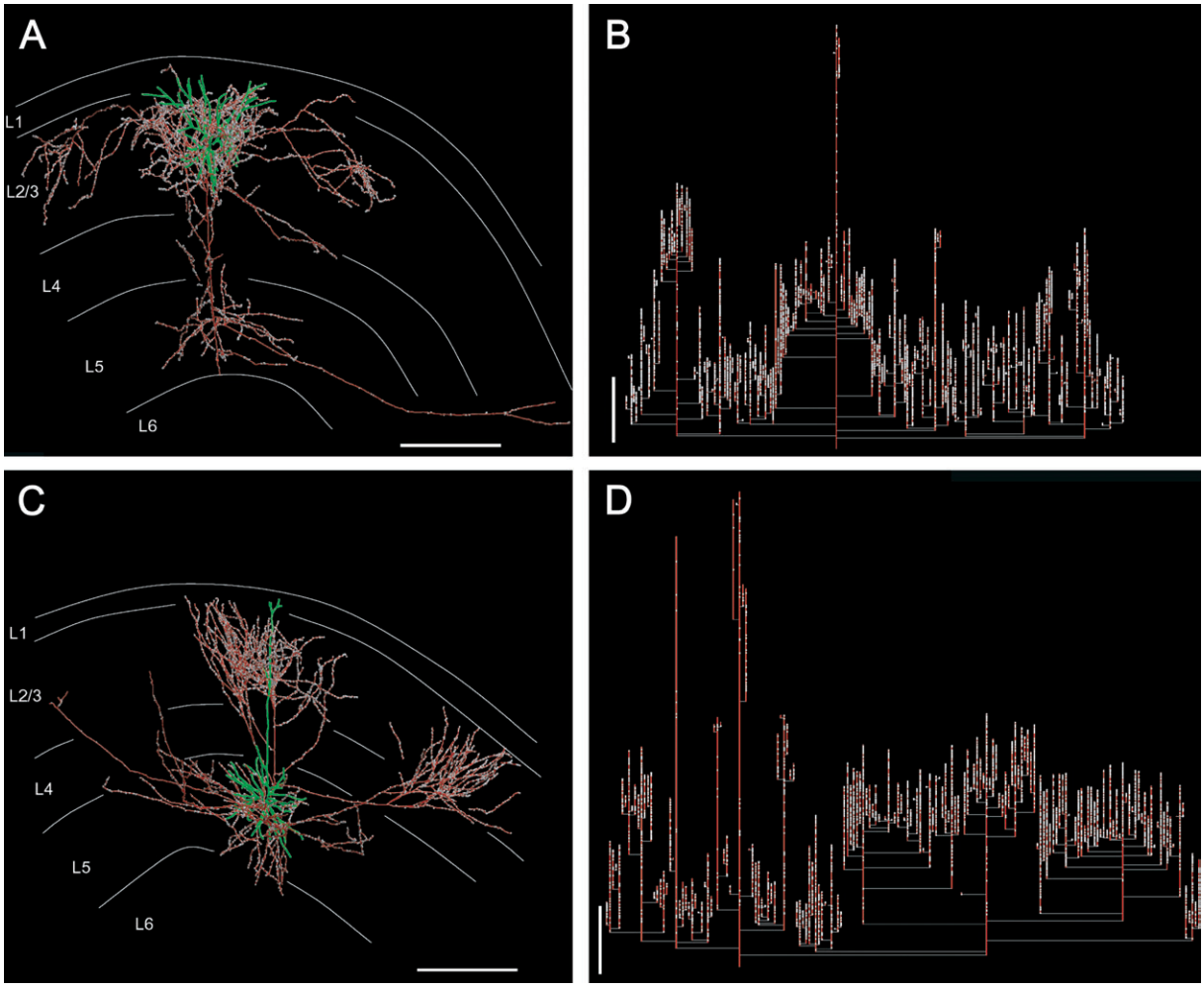

Figure 2. Coronal view of reconstructed neurons and the dendrogram of their axonal trees. For this and Figure 3 the axon is indicated in red, axonal boutons in white, dendrites in green and cortical layer borders as white lines. (*A*) Pyramidal cell in layer 2/3. Receptive field (RF) type, ocular dominance (OD) and size were as follows. Directional C ('complex') RF, OD 7, size 1.2 × 1.4°. (*B*) Dendrogram of the layer 2/3 pyramidal cell shown in *A*. (*C*) Pyramidal cell in layer 5. S1 ('simple') RF, OD 7, size 0.9 × 0.7°. (*D*) Dendrogram of the layer 5 pyramidal cell shown in *C*. Scale bars = 500 μm.

$$A_p(r_j, s_j) = \frac{|r_j - s_j|}{r_j + s_j - 2},$$

which measures at each branch point j the relative difference between the number of end collaterals r_j and s_j on the two subtrees emerging from the branch point. For $r_j + s_j < 2$ it is set $A_p(r_j, s_j) = 0$. The tree asymmetry index is the average of the A_ps. There are two extreme forms of binary trees: 'herringbone' or 'totally unbalanced' trees are fully asymmetrical and have an asymmetry index approaching 1 (for trees of high magnitude), whereas 'dichotomous' or 'totally balanced' trees, are fully symmetrical and have an asymmetry index of 0 (Fig. 1*B*). It is clear that being tree-structures, the asymmetry index of all axons that arborize in the cortex must lie somewhere between these two extremes. One interesting question is whether the asymmetry index clusters around one point, or whether it clusters at various points, perhaps correlated with the origins of the axon, e.g. the extrinsic afferents cluster at one position, the intrinsic afferents at another, or whether other factors such as cell type or laminar position of the arborization influences the topology.

Horton–Strahler Analysis

For a more detailed analysis of different parts of the dendrogram, we ordered the collaterals using the method proposed by Strahler (1952). He first introduced it in studies of the topology of river networks, where ordering begins naturally at the sources, i.e. at the smallest drainage streams that have no tributaries themselves. This centripetal ordering convention of the Horton–Strahler (HS) numbering scheme may seem counterintuitive for the description of axonal organization or growth, where the natural inclination is to begin numbering at the origin. However, as many studies show, key features about the branching behavior of river networks, dendritic trees and other natural occurring binary trees can often be characterized by only two ratios (the bifurcation and length ratio) when applying this ordering system. Capturing essential features of axonal trees in a few key numbers greatly facilitates comparisons between the axons of different types of neurons.

In this method, each collateral in a binary tree is given an order in the following way (Fig. 1*C*). The end collaterals have all order 1. If the two children of an inner collateral have order k, then the inner collateral is assigned order $k + 1$. If one child has order k and the other an order smaller than k, then the inner collateral is assigned to the larger order k. Each path formed by consecutive collaterals of the same order k is called an HS 'segment' of order k. Note again that segments can include many collaterals.

The segment with the maximum order I contains the root collateral. This number is called 'Strahler number'. A tree has to be 'pruned' $I - 1$ times in order to remove all the branches so that only the stem of the tree remains (i.e. the segment of order I in the original tree). 'Pruning' a tree is the operation that forms a new tree by 'cutting' all end collaterals. The second order segments of the old tree become the end

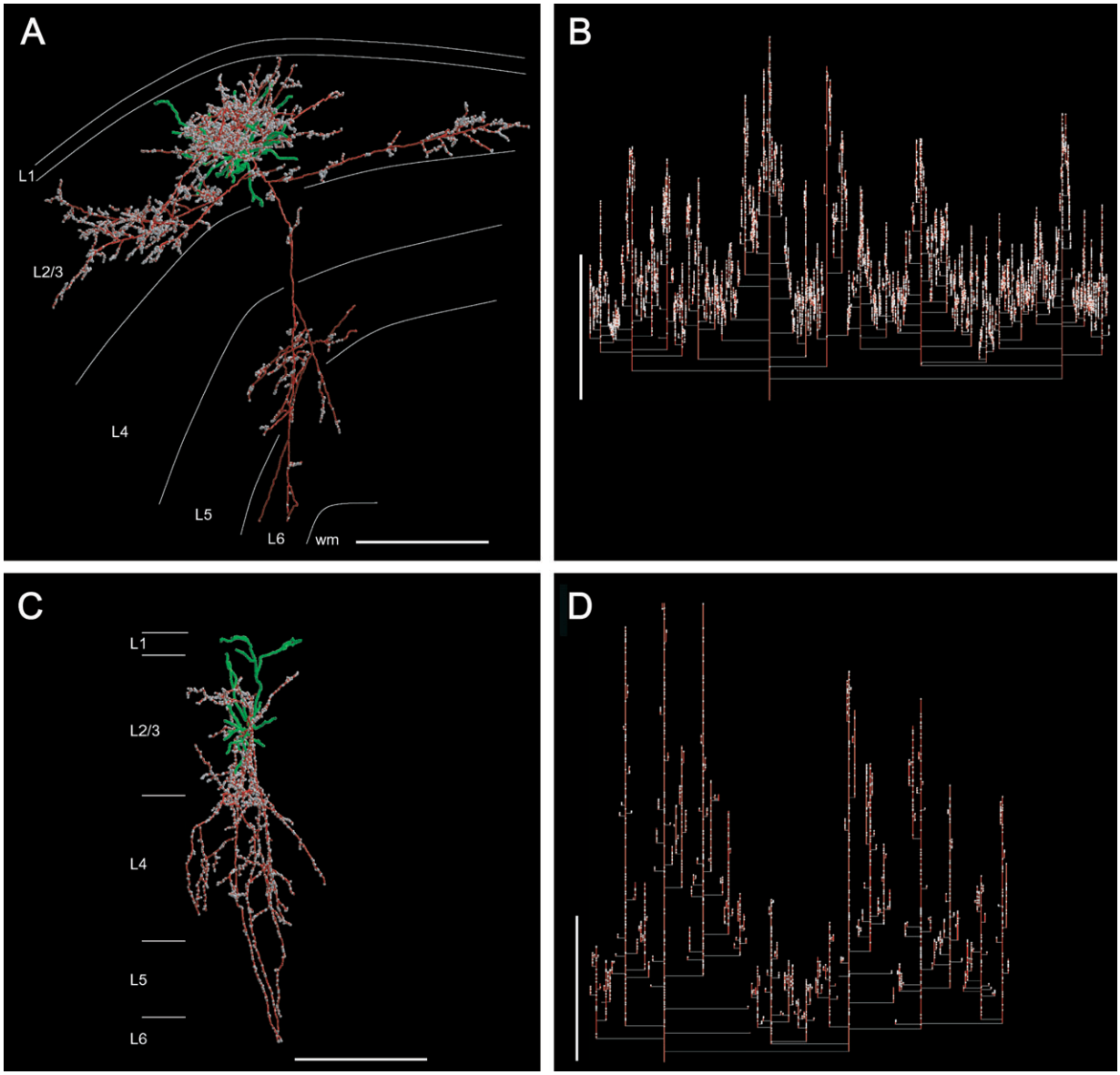

Figure 3. Coronal view of reconstructed neurons and the dendrogram of their axonal trees. (*A*) Basket cell in layer 2/3. S1 RF, OD 5, size 1.4 × 0.3°. (*B*) Dendrogram of the layer 2/3 basket cell shown in *A*. (*C*) Double bouquet cell in layer 2/3. Directional S1 RF, OD 7, size 1.1 × 2.0°. (*D*) Dendrogram of the double bouquet cell shown in *D*. Scale bars = 500 μm.

collaterals of the new tree and the numbering system is adjusted in the new tree (Fig. 1*C*,*D*).

A 'subtree of order k' consists of a segment of order k together with all the branches that emerge directly or indirectly from this segment (Fig. 1*C*). The Strahler number of this subtree is k.

Let N_k be the number of segments of order k in the tree, and L_k the average length of these segments. N_1 is the number of end collaterals, and of course $N_I = 1$. All other N_k are between these two values. The 'bifurcation ratio' of order $k \in [1, \ldots, I-1]$ is defined as N_k/N_{k+1}. This ratio measures the relative change of the number of segments as one moves from a higher order to a lower order. The 'length ratio' of order $k \in [1, \ldots, I-1]$ is defined as L_{k+1}/L_k. This ratio measures the relative change of segment length from a higher order to a lower order.

We call a binary tree 'topological self-similar' if all bifurcation ratios are similar. For a topological self-similar tree with bifurcation ratio b, the logarithm of the segment numbers N_k, plotted versus HS segment order k, forms a straight line with slope $-\log(b)$. This is an immediate consequence of the basic equation $N_k = b^{I-k} (k \in [1, \ldots, I])$. From this equation it also follows that

$$I = \frac{\log(N_k)}{\log(b)} + k$$

Fractal Dimension

We used the box-counting procedure (Mandelbrot, 1983) to assign each axonal tree, embedded in the three dimensional space, a fractal dimension. A similar procedure was used to determine the fractal dimension of dendritic trees (Caserta *et al.*, 1995). The three-dimensional space is covered with cubes of side length l_k and the number of boxes M_k which intersect with the axonal branches of the tree are counted (Fig. 8*A*). We determined M_k for the values $l_k = 20 \times 2^{k/2}$ μm, $k = 0,1, \ldots, 12$, i.e. l_k is between 20 and 1280 μm. For ideal fractal objects the points of the curve $f_k = (\log(l_k), \log(M_k))$ form a straight line and its negative slope defines the fractal dimension of the object. For natural occurring fractal objects the curve f_k forms a straight line only for a limited range. In order to find this region for an axonal tree, we first fitted a straight line (regression line) through four consecutive points $f_u, f_{1+u}, f_{2+u}, f_{3+u}$ ($u = 0,1, \ldots, 9$) of the curve and determined the slope $S(u)$ of this line

(Fig. 8*B,C*, inset). If the curve f_k is a straight line, all local slopes $S(u)$ would have the same value. We therefore looked for four consecutive local slopes $S(u)$ that had the least variance, and defined the mean of these local slopes as the fractal dimension of the axonal tree.

Branching Model

We used a Galton–Watson branching process with parameters p_{st}, p_{el} and p_{br} (Jagers, 1975) to generate randomly branching axonal trees. The parameters describe the probability of stopping growth, elongating, or branching. In order to generate a tree, we started with one segment of arbitrary length Δl = 1 μm and extended this segment by either adding a segment of length Δl or by forming a branch point and adding two children of length Δl. If the segment has elongated or branched, one or two segments are added, which we call 'end-tips'. Each of these end-tips is elongated, branched or stopped with the same probabilities p_{el}, p_{br} and p_{st}. This process produces newly formed end-tips (excluding the end-tips that stopped growing). A binary tree grows by repeating this procedure to the newly formed end-tips (Fig. 9*A*). Whether one end-tip elongates, branches or stops is assumed to be statistically independent from the elongation of other end-tips. A newly formed end-tip has exactly three possibilities for its fate (to stop growing, branch or elongate), therefore

$$p_{st}+p_{el}+p_{br}=1 \tag{1}$$

(these probabilities are fixed parameters). The tree will finally stop growing (because no more end-tips are formed) if the following relation holds (Jagers, 1975)

$$p_{el}+2p_{br} < 1 \tag{2}$$

We enforced this relation so that the tree could not grow infinitely. Here we focus on the probabilities p_{st}, p_{el} and p_{br} for which relation 2 holds, and thus avoid the need to introduce explicit stopping rules that prevent the tree from growing infinitely long. For convenience we merge (1) and (2) into the form:

$$p_{st}=1-p_{el}-p_{br},\ 0 < p_{br} < \frac{1-p_{el}}{2} \tag{3}$$

The probabilities p_{st}, p_{el} and p_{br} completely determine the distribution of branch lengths of the grown tree. The probability that a given end-tip grows by Δl is p_{el} and that the end-tip stops growing (because the end-tip forms a branch point or stops growing) is $1-p_{el}$. Thus, the probability that a branch (chain of segments between branch points or between branch-points and end-tips that stopped growing) has length $l = \Delta l \cdot k$ is

$$f_{p_{el}}(k)=(1-p_{el})\cdot p_{el}^{k} \tag{4}$$

where k is a natural number.

Results

A total of 39 axons were reconstructed completely and measured in 3D. Four examples of the reconstructions of different neurons whose major axonal arbor is in layers 2 and 3 are shown in Figures 2*A,C* and 3*A,C*, together with examples of the dendrogram of the axon and the distribution of the boutons (Figs 2*B,D* and 3*B,D*). The neurons are shown in the transverse view, with dendrites coded green, axons red, and synaptic boutons in white. The thickness of the dendrites and axons is not represented. In the dendrogram the cell body is the origin. For clarity, the collaterals (indicated by red vertical lines) have been displaced horizontally and the white lines simply indicate the branch points. The receptive field types of these neurons and other properties are reported in the legends to Figures 2 and 3. Twenty-three neurons had spiny dendrites, 13 neurons had smooth dendrites, and the remaining three were thalamic axons of the lateral geniculate nucleus (LGN). The breakdown according to layers and subtype (pyramid, basket, double bouquet etc.) is given in the legend to Figure 4.

Number and Length of Collaterals

Calculations of average axon lengths in neocortex have been based mainly on estimates of the percentage of neuropil occupied by axon-like profiles (Foh *et al.*, 1973; Braitenberg and Schüz, 1991). Here we could measure the total lengths (i.e. the summed length of the axon collaterals in the tree) of individual axons directly. These ranged between 11.7 and 125.5 mm (average length 41.3 ± 20.9 mm, mean ± SD; Fig. 4*A*). The axonal arborization of smooth cells were restricted to a much smaller volume than spiny cells and thalamic afferents and this was reflected in their average total axonal length (31.8 ± 11.7 mm, range 11.7–52.1 mm), which was smaller than that of spiny cells (47.4 ± 23.8 mm, range 18.7–125.5 mm) and thalamic afferents (35.5 ± 11.0 mm, range 27.0–48.0 mm). Only the basket cells in layer 2/3 (36.0 ± 2.7 mm, range 32.9–37.9 mm; n = 5) had a total axonal length comparable to spiny cells. The biggest axonal arbors in terms of total length were made by the pyramidal cells in layers 2 and 3 (3/5) and one layer 5 pyramidal cell, which had total axon lengths in excess of 60 mm.

The number of collaterals of the axonal trees varied widely, from 103 to 1403 (Fig. 4*B*). Although their average total axon length was greater, spiny cells and thalamic afferents tended to have fewer axon collaterals than the smooth cells. Basket cells in layer 2/3 had about twice as many collaterals as the maximum number of collaterals seen for spiny neurons and thalamic axons. The average number of collaterals of the smooth cells was 803 ± 329 (range 325–1403), that of the spiny cells and thalamic afferents 306 ± 140 (range 103–641) and the collateral lengths were correspondingly different for these two groups (Fig. 4*C*). The smooth cells had median lengths for their collaterals that varied between 23 and 50 μm (30 ± 7 μm). The spiny cells had median lengths ranging from 64 to 167 μm (104 ± 22 μm). The thalamic afferents had intermediate collateral lengths, with the median ranging from 39 to 50 μm (43 ± 6 μm). The longest collaterals were found on a layer 6 pyramidal cell whose axon was restricted to layer 6 (see Fig. 4*C*) and a star pyramidal cell of layer 4 with diffuse branching pattern (p4). The star pyramid cell had the lowest number of collaterals of any cell.

Length Distribution of Collaterals

The distribution of collateral lengths over the entire axonal tree was roughly similar for neurons within the group of spiny neurons, smooth neurons and thalamic afferents. By inspection, the distributions are approximately exponential, but have a relative lack of very short (<~20 μm) collaterals. Such short collaterals would easily be seen in the light microscope, so their unexpectedly low occurrence is not an artifact of reconstruction. Beyond this lack of very short collaterals, smooth neurons and thalamic afferents had a higher proportion of short (<~50 μm) collaterals than spiny neurons, reflecting the results we found for the median collateral lengths (Fig. 4*D–F*).

Tree Magnitude and Length of End-collaterals

The end collaterals had median lengths that were generally larger than the lengths of the inner collaterals (absolute difference 28 ± 40 μm, range of differences between 19 and 203 μm). An extreme example was the star pyramidal cell of layer 4 (p4), where the median length of the end collaterals was ~200 μm longer than that of the inner collaterals. However, for many neurons (24/39) the absolute difference was <20 μm and the two distributions were often (23/39) not significantly

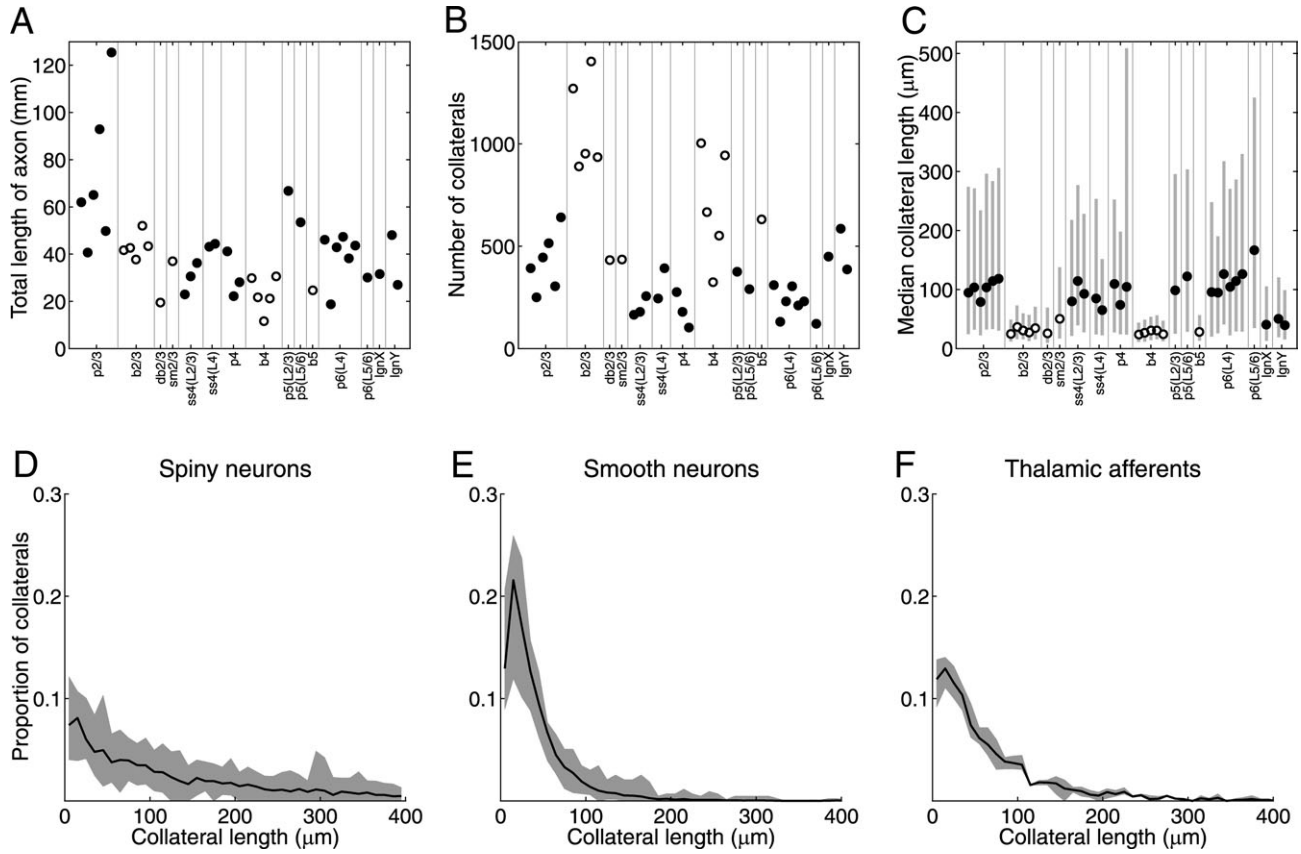

Figure 4. Metrical characterization of the axon collaterals. (*A*) The total axonal length of individual cells was computed. (*B*) The total number of axon collaterals are shown for each cell. (*C*) Median of the collateral lengths of each cell. Gray bars indicate the 20th and 80th percentiles of the distribution of collateral lengths. (*A–C*) open circles indicate smooth cells, closed circles spiny cells and thalamic afferents. Abbreviations: p2/3, p4, p5, p6, pyramidal cells in layer 2/3, 4, 5 and 6; ss4, spiny stellate cells in layer 4. Pyramidal cells in layer 5 and 6 and spiny stellate cells were sub-classified depending on the preferred layer of innervation (indicated in parenthesis in the labels). Lgn, X-type thalamic afferent (lgnX) and Y-type (lgnY); b2/3, b4, b5, basket cells in layer 2/3, 4 and 5; db2/3, double bouquet cell in layer 2/3; sm2/3, unclassified smooth cell in layer 2/3. (*D–F*) Histogram of the number of collateral lengths for the spiny neurons (*D*), the smooth neurons (*E*) and the thalamic afferents (*F*). The shaded area indicates the maximum and minimum number of collaterals per bin for the different cells in a class. The solid line in each inset indicates the bin-wise median. Bin size is 10 μm. Median values of the pooled collateral lengths were 98.8 μm for the class of spiny neurons, 28.5 μm for the smooth neurons and 45.0 μm for the thalamic afferents.

different (significance level 0.01). The number of end collaterals is referred to as the 'magnitude' of the tree. The total number of collaterals in the tree is twice the magnitude minus 1 (see Materials and Methods). The magnitude and the mean length of the end collaterals will be used in the topological and HS analysis of the axonal trees and are shown in Figures 5 and 6.

Topological Analysis

In order to make an objective comparison of the axonal branching pattern of the 39 neurons, we applied a number of well-established methods to define the topology of the axonal trees. However, while these methods are frequently used to describe natural structures (e.g. rivers and root systems), they are rare in applications to neurons and thus require some introduction. We apply them here, because these topological methods offer compact descriptions based on quantitative measures of some key aspects of the branching patterns of axons that are independent of the embedding in the three dimensional space. Thus, topological analysis provides simple and direct comparisons between the different axon types that goes beyond the obvious differences of axonal innervation patterns, such as the differential selection of cortical layers or the formation of axonal patches. Constancies of organizational form hidden from normal metrical analyses may be revealed by topological analyses.

Topological Depth, Height, Exterior Path Length and Magnitude

The 'depth' of a particular end collateral is a convenient measure of the number of collaterals (including the root collateral and the end collateral itself) along the shortest path between the root and the given end collateral (see Fig. 1*A*). The maximum depth of the end collaterals considered over the whole arbor is called the 'height'. The average height of all axons was 21 ± 6 (range 12–37). Although the overlap was large, the spiny neurons had a smaller height (18 ± 4, range 12–24) than the smooth neurons (25 ± 7, range 17–37) or thalamic afferents (25 ± 3, range 22–27).

A measure of the degree of collateral branching is given by the sum of the depths of all the end collaterals: this sum is referred to as the 'exterior path length'. The average exterior path length of the whole population of cells was 2999 ± 2420 (range 420–10467). It was smallest for the spiny neurons, 1624 ± 936 (range 420–4141), followed by the LGN axons with 3426 ± 486 (range 2869–3766). The largest exterior path length was formed by the smooth neurons, with 5333 ± 2706 (range 1862–10467).

Axonal trees with similar 'magnitude' (the number of end collaterals) had similar height and exterior path length (Fig. 5*A*,*B*). The dependence on the magnitude ν_0 (or

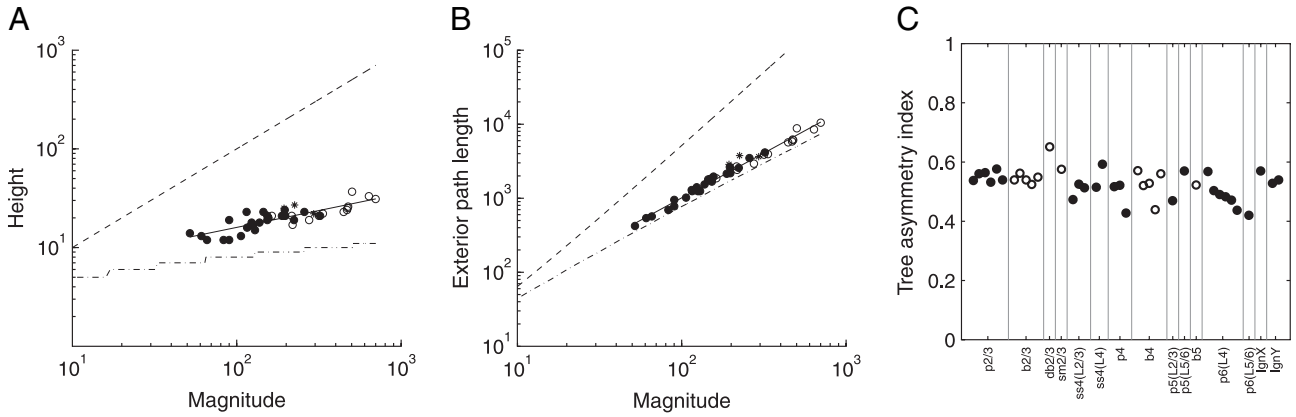

Figure 5. Topological characterization of the axon collaterals. (*A*) Log–log plot of height of an axonal tree as a function of magnitude. Dashed lines indicate the maximum and minimum height of all binary trees of a given magnitude. Thin black line indicates regression line through data points ($r = 0.83$, $a = 0.52$, $b = 0.34$). (*B*) Log-log plot of exterior path length of an axonal tree as a function of magnitude. Dashed lines indicate the maximum and minimum exterior path length of all binary trees of a given magnitude. Thin black line indicates regression line through data points ($r = 0.99$, $a = 0.58$, $b = 1.21$). (*A*, *B*) Open circles indicate smooth cells, closed circles spiny cells and stars indicate thalamic afferents. (*C*) Asymmetry index of each axonal tree. The tree asymmetry index equals zero when on average at each bifurcation the two subtrees have an equal amount of end collaterals (i.e. maximally symmetry) and approaches 1 when at each bifurcation one of the subtrees is an end collateral (maximally asymmetry).

equivalently on the number of end collaterals) of the height and the exterior path length can be described reasonably well by a power function of the form $\alpha \cdot v_0^{\beta}$. Based on the regression lines in Figure 5*A*,*B*, we estimated α and β. For the height we got $\alpha = 3.3$ and $\beta = 0.34$, for the exterior path length $\alpha = 3.80$ and $\beta = 1.21$. The dashed lines in Figure 5*A*,*B* indicate the maximum and minimum height and the maximum and minimum exterior path length for trees of a given magnitude.

Figure 5*C* provides a comparison of the degree of topological asymmetry of the axonal trees. Intuitively, the tree asymmetry index is an average measure of the size difference between the two subtrees that emerge from the branch points of the tree. For example, a herringbone tree (Fig. 1*B*) of high magnitude is maximally asymmetric (i.e. has an index of 1), because for any branch point one emerging subtree is very small (consisting of one end collateral), while the other emerging subtree is very big (having many end collaterals). In contrast, a dichotomous tree (Fig. 1*B*) is maximally symmetric (i.e. has an index of 0), because for any branch point the two emerging subtrees have an equal amount of end collaterals. Despite their differences in size and complexity, the asymmetry index is very similar for all the axonal trees (0.53 ± 0.05, range 0.42–0.65, Fig. 5*C*). Typically, one subtree emerging from a branch point of an axonal tree has about three times as many end collaterals as the other subtree.

Horton–Strahler Analysis

The analysis of the collateral length showed that end-collaterals are typically shorter than the inner collaterals. This indicates that axon collaterals form a heterogeneous population that divided into classes of different metrical and topological properties. The topological and metrical measures applied so far are global in the sense that they do not distinguish collaterals of different groups. We therefore use here the Horton–Strahler method to order collaterals of an axonal tree into a hierarchy and to compare the different levels. Although 'collateral' takes a slightly different meaning in this context (and is called 'segment'), in the analysis we basically compare the change in segment number and segment length between the different levels, and also compare these changes between the different axonal trees.

The Strahler number I is a measure of the degree of branching of a tree. It is derived by determining how many times the tree has to be pruned in order to cut off all branches. Each 'pruning' removes all the end collaterals. The second order collaterals of the old tree become the end collaterals of the new tree and the numbering system is adjusted in the new tree (Fig. 1*C*,*D*). The more 'complex' the branching, the higher the Strahler number. For the axonal trees of smooth cells, the Strahler number ranged between 6 and 7 with one exception, a basket cell in layer 4, where $I = 5$. Spiny cells and thalamic afferents had Strahler numbers between 5 and 6. (It should be noted that the thalamic afferent root was taken as the entry point to the cortical grey matter and not the origin of the axon in the thalamus, where additional branching might occur.) With one exception, the spiny cells of type p2/3 had a Strahler number of 6, and, again with one exception, layer 6 pyramidal cells had a Strahler number of 5.

In the Horton–Strahler (HS) numbering scheme, the end collaterals are the first order segments of the axonal tree for which the number (N_1) and average length (L_1) are shown in Figure 6*A*,*B*. The number of first order segments (the end collaterals) is linearly related to the total number of collaterals. This number varied widely, from 54 for the star pyramid of layer 4, to 702 for a layer 3 basket cell. As might be expected, the average length of end collaterals dominates the distribution and thus is close to the median length of all collaterals (Fig. 4*C*).

Bifurcation Ratio

A basic property of binary trees is that the number of segments of a given order increases as the order number decreases. The topological measure of the relative increase of segments from a higher to a lower order is termed the bifurcation ratio. More exactly, the bifurcation ratio of order k is the ratio N_k/N_{k+1} of the number of segments of order k and $k + 1$. Bifurcation ratios are always > 2, but otherwise unlimited (in theory). For many natural occurring trees [including dendrites of rat neocortex (MacDonald, 1983)] the bifurcation ratios are rather independent of the order and have a value between 2 and 5.

The first and second order bifurcation ratios of the reconstructed axonal trees are very similar (Fig. 6*C*). The first order bifurcation ratio (N_1/N_2, circles) ranges between 2.8 and 4.5

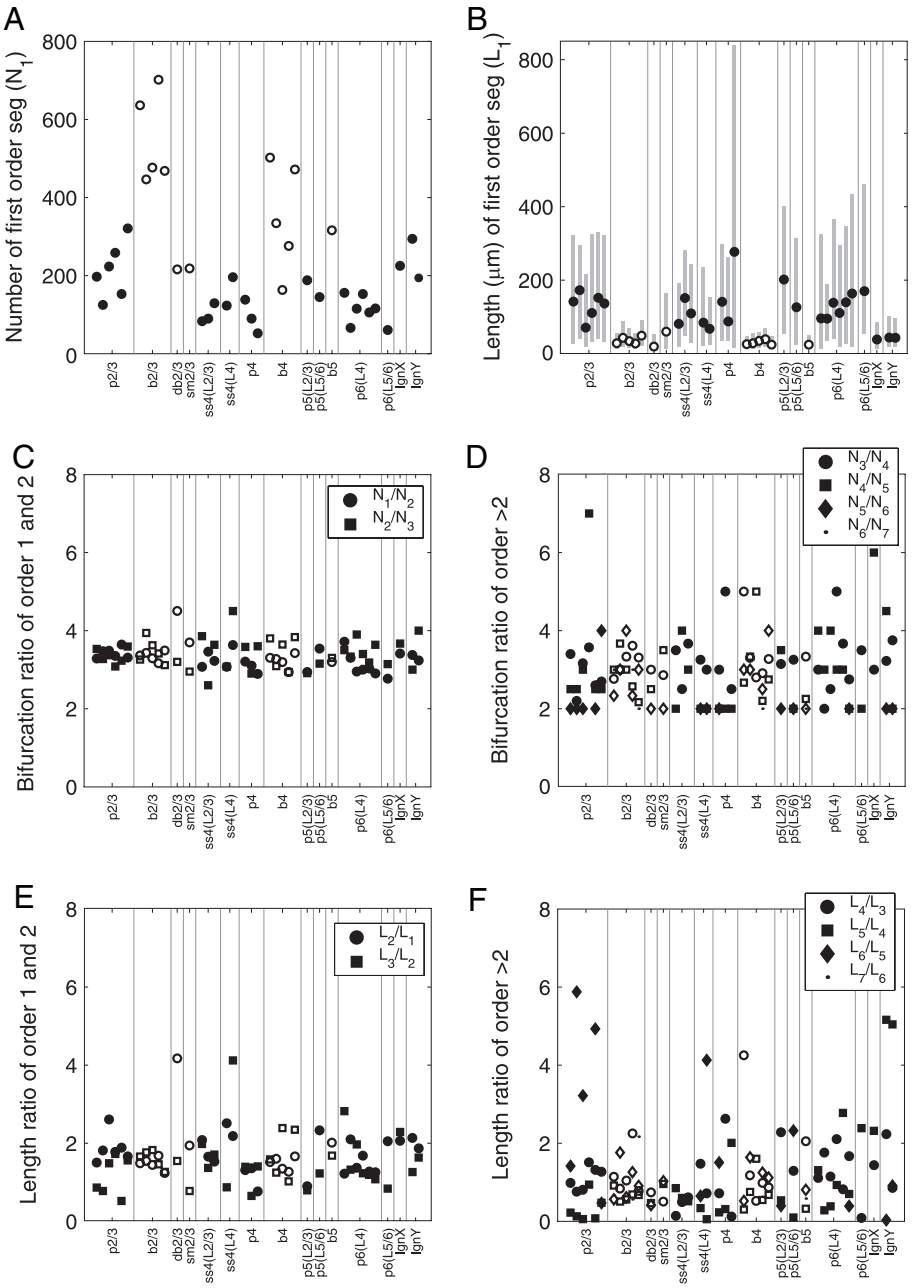

Figure 6. Horton–Strahler analysis of axonal trees. (*A*) Number of first order segments (i.e. number of end collaterals or magnitude) of each axonal tree. (*B*) Mean length of the first order segments for each axonal tree. Gray bars indicate the 20th and 80th percentiles of the distribution of first order segment lengths. (*C*) First and second order bifurcation ratio for each axonal tree. (*D*) Higher order bifurcation ratios. (*E*) First and second order length ratio for each axonal tree. (*F*) Higher order length ratios for each axonal tree.

(mean 3.3 ± 0.3), the second order ratio (N_2/N_3, squares) between 2.9 and 4.5 (3.4 ± 0.4). For the neurons with dissimilar bifurcation ratios, no clear pattern could be observed concerning the size relation. For example, the bifurcation ratio of order 1 was bigger than the bifurcation ratio of order 2 in the case of the double bouquet cell, but smaller for one of the spiny stellate cells which had its major axonal arborization within layer 4.

The bifurcation ratios of higher orders are more varied, but the vast majority of the ratios (92%) still lie between 2 and 4 (Fig. 6*D*). The mean of the pooled ratios of order > 2 is 2.9 ± 0.9 (range 2.0–7.0). The mean of the pooled ratios of all orders is 3.1 ± 0.8 (range 2.0–7.0).

We also estimated the common bifurcation ratio b, by plotting for each tree the number of segments of order $k + 1$ against the number of segments of order k (Fig. 7*B*). The points lie on a straight line through the origin, which confirms that our entire sample of axons (both spiny and smooth) have similar bifurcation ratios ($b = 3.32$, $r = 0.99$). This result suggests that all the axons are topologically self-similar. Indeed, Figure 7*A* demonstrates that, despite the variances in higher order bifurcation ratios mentioned above, the overall relationship between $\log(N_k)$ and order k for individual axons is linear. Furthermore, the HS index predicted by $\log(N_1)/\log(b) + 1$ is in good agreement with the observed values (Fig. 7*C*).

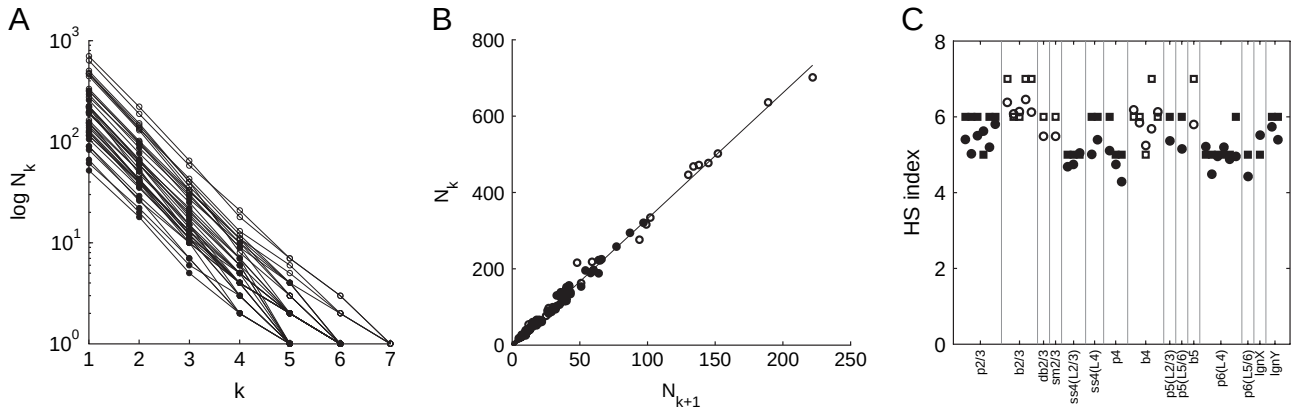

Figure 7. Topological self-similarity of axonal trees. (*A*) Test for topological self-similarity. For each axon the logarithm of the number of segments of HS order k is plotted against k. The approximately straight line formed by the dots of each tree indicates that its bifurcation ratios are similar, i.e. the tree is topological self-similar. This bifurcation ratio is given by the exponential of the negative slope of the straight line. The similarity of the slope for the different trees suggests a common bifurcation ratio b for all trees. Closed circles: spiny neurons and thalamic afferents. Open circles: smooth neurons. (*B*) Estimation of the common bifurcation ratio b. For each tree the number of segments of order $k + 1$ is plotted against the number of segments of order k. If all trees had exactly the same bifurcation ratio b, the points would lie on a straight line through the origin with slope b. We estimated b by the slope of the regression line fitted through the points ($r = 0.99$), which revealed $b = 3.32$. Closed circles: spiny neurons and thalamic afferents. Open circles: smooth neurons. (*C*) Verification of estimated bifurcation ratio b. For each tree, the Strahler index I (squares) was compared with the value $\log(N_1)/\log(b) + 1$ (circles), where b as estimated in *B*. If the trees were topologically self-similar with a common bifurcation ratio b, the two numbers are equal for each tree. Closed symbols: spiny neurons and thalamic afferents. Open symbols: smooth neurons.

Length Ratio

The length ratio measures the relative increase of the length of the collaterals from a lower to a higher order. The length ratio of order k is the ratio L_{k+1}/L_k of the average length of segments of order $k + 1$ and k. Length ratios can take any value >0. For naturally occurring tree structures [including dendrites of rat Purkinje cells (MacDonald, 1983)] the length ratio is relatively independent of the segment order and typically has values between 1 and 2.

For the reconstructed axonal trees, the average length ratios of order 1 (L_2/L_1, Fig. 6*E*, circles) is 1.7 ± 0.6 (range 0.8–4.2). For the second order length ratio (L_3/L_2, Fig. 6*E*, squares) the average is quite similar, 1.5 ± 0.7 (range 0.5–4.1). Most ratios are >1. For the first order ratios this means that the end collaterals (the segments of order 1) are typically smaller than the second order segments. As with the bifurcation ratios, no clear pattern was observed concerning the size relationship of the first and second order length ratios [i. e. Fig. 6*E*, db2/3, ss4(L4)].

As with the bifurcation ratio, the higher order length ratios are more varied (1.2 ± 1.1, range 0.03–5.9, Fig. 6*F*). The average of the pooled length ratios of all orders is 1.4 ± 1.0 (range 0.0–5.9). The average length of segments of order $k + 1$ and the average length of segments of order k, pooled for all neurons and all orders, did not correlate ($r = 0.39$). Thus, in contrast to the branching ratio (Fig. 7*B*), there is no global length ratio that applies to all axons and all orders.

Fractal Analysis

Whereas HS methods measure the topological 'complexity' of a tree in terms of the number of times a tree can be pruned, fractal methods measure its dimensional 'complexity'. The higher the fractal dimension of the tree, the bushier it appears (Fernández and Jelinek, 2001). To the extent that axons are fractal at all, they have the fractal property of self-similarity. Natural objects are not ideal mathematical objects, and so they are not expected to exhibit exact fractal self-similarity. Nevertheless, they may show some degree of self-similarity over a limited range of scales (in our case, spatial scale). A large axonal tree with constant HS bifurcation and length ratios should display some scale invariance (Tarboton *et al.*, 1988). Although our axons have quite strong fluctuations of higher order branching and length ratios, we expected to find evidence of this invariance by fractal analysis.

We used the box-counting algorithm to determine the fractal dimension of axonal trees embedded in their three dimensional space (Fig. 8*A,B*). The fractal dimension of axons of all cells was rather similar, with a slight tendency of smooth cells to be higher (Fig. 8*B,C,D*). Spiny cells and thalamic afferents have an average fractal dimension of 1.5 ± 0.1 (range 1.2–1.7), for smooth cells it is 1.7 ± 0.2 (range 1.4–1.9). Some neurons show a fairly straight line in the box-counting approach (Fig. 8*B,C*), indicative of fractal self-similarity. However, we also found axons for which the curve $l \rightarrow M(l)$ hardly contained a straight segment (≈7/39), indicating a lack of fractal self-similarity.

Growth Model

Apart from some specific lengthening of some high-order axonal segments, the metrical and topological aspects of the axonal data can be described by a simple growth model. The model we used is a Galton–Watson branching process, which is one of the simplest and best understood (Jagers, 1975). A tree is grown (Fig. 9*A*) by repeatedly elongating its end-tips by 1 μm (with probability p_{el}) or by branching the end-tips into two new branches of length 1 μm (with probability p_{br}), causing two new end-tips. It is also possible to stop the growth of an end-tip (with probability p_{st}).

Estimation of the Parameters p_{st}, p_{el} and p_{br} for the Reconstructed Trees

To test whether the Galton–Watson branching process is a reasonable model of the terminal branching of axonal trees, we estimated p_{st}, p_{el} and p_{br} for the two major subdivisions of the axonal types — those originating from spiny cells and thalamic afferents, and those of smooth cells. Note that because of relation (1) it is enough to estimate p_{el} and p_{br}. We modeled only the growth of the terminal arbors (i.e. subtrees of order 2 or 3), which constitute most of the axon. We did not model the

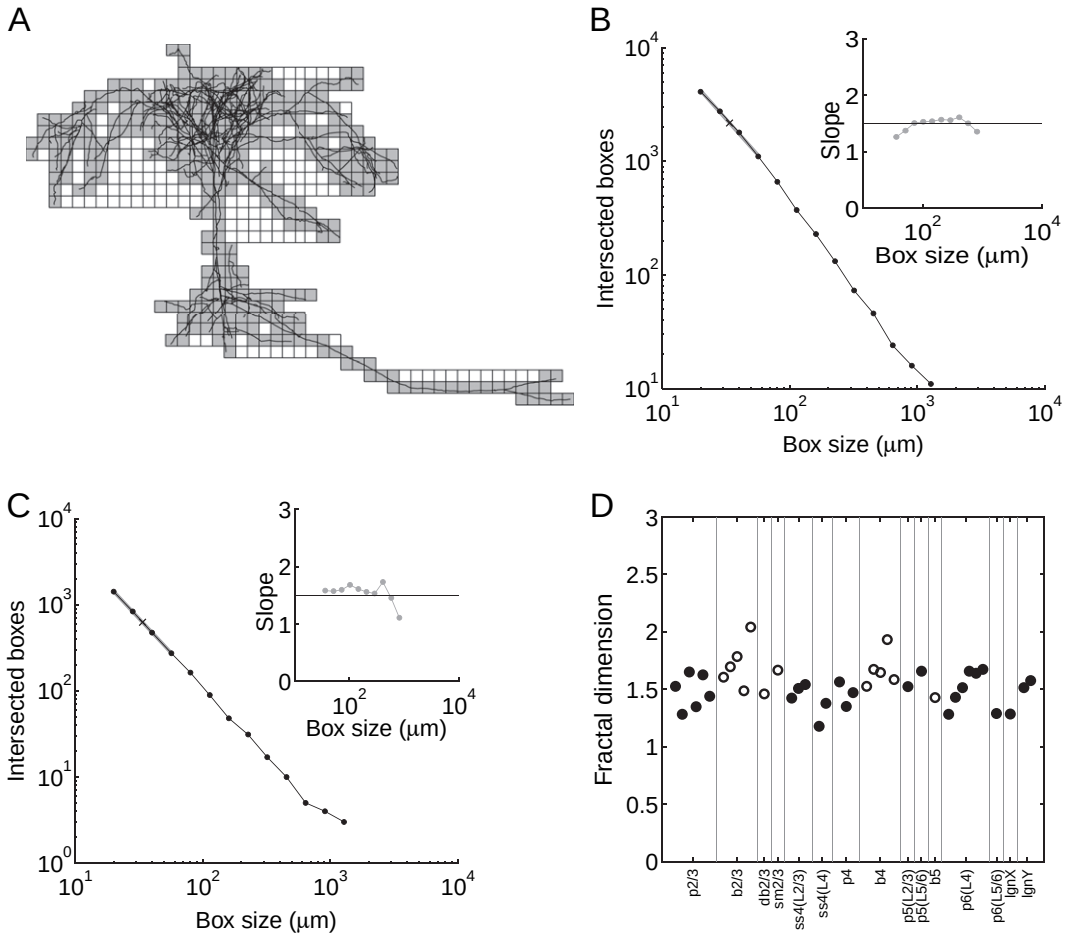

Figure 8. Fractal dimension of 3D axonal trees. (*A*) Box-counting method was used to determine the fractal dimension. The axon of a layer 2/3 pyramidal cell was covered with cubes (side-length 60 μm). Shown is the coronal view of the axon, the cubes (which appear as squares in this perspective) that cover the axon and the cubes that intersect with axonal branches (gray squares). (*B*) Number of cubes intersecting with the axonal branches (of the cell in *A*) is shown in log–log space as a function of cube side-length. Inset: negative local slope of the curve (indicated in gray) measured by the regression line through four consecutive points in the curve. The first slope is indicated by a gray bar in the main figure. The fractal dimension of the axonal tree is the negative slope of an approximately constant region of the gray curve. (*C*) Similar to *B*, but for a layer 4 basket cell axon. (*D*) Axonal fractal dimension for each neuron.

main axonal trunks because they are rather few in number and varying considerably in length (see Figs 2 and 3), thus compromising any statistical comparison with the simple Galton–Watson branching process. We described each of the two axonal types (spiny and smooth) by the histogram of branch length ($f_{p_{el}}(k)$), the first bifurcation and length ratio, and for the subtrees of order 3 also the second order bifurcation and length ratio (Fig. 9*B*,*C*).

In order to estimate p_{el}, we fitted for each population the function $f_{p_{el}}$ to the histogram of branch length (equation 4). Reasonable fits were obtained for p_{el} = 0.9927 (spiny population) and p_{el} = 0.9780 (smooth population). The best fit was found by minimizing the least square error using the Levenberg–Marquardt algorithm. In order to estimate p_{br} we picked values in the interval

$$0 < p_{br} < \frac{1 - p_{el}}{2}$$

because the distal trees have to stop growing at some point (see equation 3). For each picked value p_{br} we produced 10 000 trees and determined the first and second order bifurcation and length ratios of the generated trees with Strahler number 2 or 3. The value p_{br} for which the resulting ratios were closest to the observed ratios for the population of distal subtrees was selected (spiny neurons: p_{br} = 0.0025, smooth neurons p_{br} = 0.0074). A comparison shows that for both groups, spiny and smooth neurons, parameters p_{el}, p_{br} and p_{st} exist that reproduce to a good approximation the branching ratio, bifurcation ratio and branch length distribution of the distal subtrees of the reconstructed axonal trees (Fig. 9*B*,*C*).

Discussion

Our results show that there are strong metrical and topological similarities between the axons of recognized neuron types, despite large differences in the appearances of the axonal arbors of these many different types of cortical neurons. These similarities are intriguing, especially in light of the differences in the appearance of the axons when viewed in the conventional 2D format (Figs 2*A*,*C* and 3*A*,*C*). The laminar specificity of the axons and differences in the lateral and vertical extents of the axons is clearly a major cue to distinguishing between different neuronal types. However, this 2D format does not give much insight into the branching patterns of the axons. The dendrograms illustrated in Figures 2*B*,*D* and 3*B*,*D* are much more revealing of the qualitative similarities and differences in branching patterns of different axons. While classifications of neuronal types have

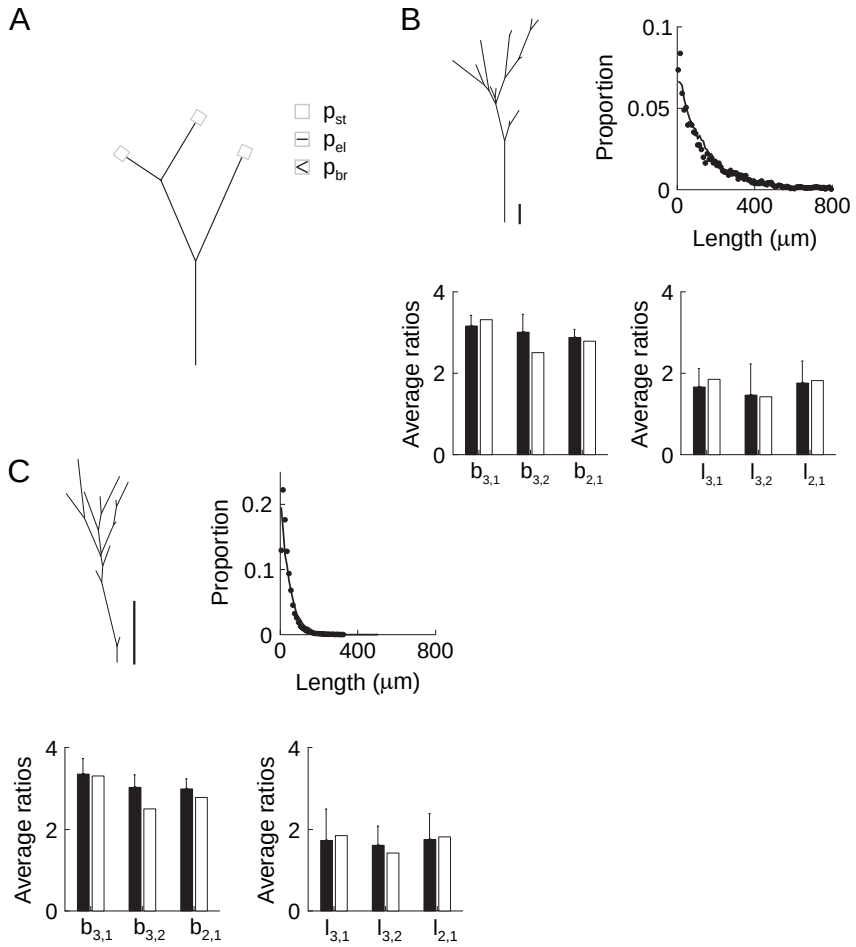

Figure 9. Random branching model of the distal part of axonal trees. (*A*) Branching model (Galton–Watson branching process). Each end-tip (squares) grows and forms new end-tips by adding a segment of length 1 μm (with probability p_{el}) or by forming a branch point and adding two segments of length 1 μm (with probability p_{br}). Each end-tip can also stop growing (with probability p_{st}). (*B*) Comparison of randomly generated trees with the distal subtrees of axons of spiny neurons. Upper left panel: example of a randomly generated tree with Strahler number 3 ($p_{st} = 0.0048$, $p_{el} = 0.9927$, $p_{br} = 0.0025$). Branching angles were arbitrary chosen (60°). Ten thousand trees were produced: 641 trees had Strahler number 3; 2678 trees had Strahler number 2; and 6624 had Strahler number 1. Upper right panel: histogram of branch lengths of the randomly generated trees with Strahler number 3 (solid line). For comparison, the histogram of pooled branch length of the reconstructed axonal subtrees with order 3 of spiny neurons is also shown (dots). Bottom left panel: first ($b_{2,1}$, $b_{3,1}$) and second ($b_{3,2}$) order bifurcation ratios of randomly generated trees with Strahler order 2 and 3 (white bars). The corresponding ratios of the reconstructed axonal subtrees with order 2 and 3 of spiny neurons are shown in black bars. Bottom right panel: First ($l_{2,1}$, $l_{3,1}$) and second ($l_{3,2}$) order length ratios of randomly generated trees with Strahler order 2 and 3 (white bars). The corresponding ratios of the reconstructed axonal subtrees with order 2 and 3 of spiny neurons are shown in black bars. (*C*) Comparison of randomly generated trees with the distal subtrees of axons of smooth neurons ($p_{st} = 0.0146$, $p_{el} = 0.9780$, $p_{br} = 0.0074$). Ten thousand trees were produced: 641 trees had Strahler order 3; 2643 trees had Strahler order 2; and 6653 trees had Strahler order 1. The description of the four panels is similar to *B*. Scale bars = 100 μm.

proceeded well without using quantitative methods, any deeper consideration of the structure of axons requires more systematic and quantitative methods, some of which we have applied here.

Simple measures, such as the lengths of axons and the order, number, and length of branches are needed, since there are so few direct measurements of filled cortical axons in the literature. Here the 2D dendrogram is invaluable as a means of organizing and representing the axonal tree. In the dendrogram, the axonal branches and their relative lengths, and the tree-like structure of the axons are readily apparent, quantitative measurements are easily made, and the topology of the axonal trees can be characterized.

Similarity of Branching Rules

Our topological (Fig. 5) and HS analysis (Fig. 6) show that all the axons occupy a relatively restricted region of the possible parameter space. Within this sub-space we could not detect a consistent and distinct signature for the different cell-types. For example, the axonal tree height and exterior path length tended to be smaller for the smooth neurons than the spiny neurons, suggesting that a topological distinction between these two classes might be possible. However, both these numbers are strongly correlated with the magnitude of the tree (Fig. 5*A*,*B*) because, for trees of a given magnitude, the height and exterior path length must fall within a range whose lower and upper limits themselves increase with magnitude (Fig. 5*A*,*B*, lower stippled lines). Of course, within this range, the values could still be arbitrary. But they are not. Instead, for all axons examined, the dependence on the magnitude can be described by just two functions; one for the height and the other for the exterior path length (Fig. 5*A*,*B*). This surprising regularity suggests that the axonal branching pattern of all neurons, spiny or smooth, is related and follow similar branching (growth) rules. This hypothesis is further strengthened by the analysis of the HS bifurcation and length ratios.

Horton–Strahler Analysis

The HS method has been applied successfully to both physical and biological tree-like structures (for example, river networks, blood vessels, and trees). The HS ordering was useful for our application, because it expresses the hierarchy between segments based on patterns of branching, and therefore allows us to investigate axonal structure on a finer level. In the original HS application of river systems, a higher order segment provides a branch that drains equivalent lower order (more peripheral) tributaries. In the case of the axons, the higher order segment can be interpreted as a source branch that gives rise to (possibly many) hierarchically equivalent lower order branching patterns. The highest order segment is the trunk whose origin is at the soma.

The HS 'bifurcation' ratio measures the relative change in the number of hierarchically equivalent segments when moving distally from one segment order to the next. The length ratio measures the relative change in average segment length when moving distally from one segment order to the next lower, and so indicates the degree of extension of the tree. The HS method has proved useful, because the bifurcation ratios and length ratios of natural tree-like structures turned out to be relatively insensitive to segment order, i.e. natural trees can often be described by a constant length ratio and a constant bifurcation ratio, which indicates topological self-similarity.

We found that the bifurcation ratios of all orders and all investigated neurons can be reasonably well described with one global bifurcation ratio (Fig. 7*A,B*). Thus each axonal tree is, to a first approximation, topological self-similar. This offers a great simplification in that the number of segments of similar order is fully determined by only three variables: the Strahler number, the global bifurcation ratio, and the segment order (see Materials and Methods). In fact, the number of segments of similar order is only dependent on the Strahler number and the segment order, because the bifurcation ratio applies globally to all axons. In particular, the Strahler number is the only determinant of the number of end-collaterals (end-collaterals have always segment order 1), and therefore of the total number of axonal branches that an axonal tree can form (Fig. 7*C*).

The situation for the length ratio was different in that we did not discover a global length ratio that applied to all axons and all segment orders. Nevertheless, the first and second order length ratios are also rather similar for the different cells (Fig. 6*E*), fluctuating around a mean value 1.6. The global bifurcation ratio was 3.3. These values are within the range for many naturally occurring tree-like structures (MacDonald, 1983).

These observations suggest that the topology of axons may be dominated by fundamental principles of construction [for example, simple growth rules that optimize the distribution of metabolic materials through a space-filling branching tree (Changizi, 2001)], rather than by the need to make connections to very specific targets.

Of course, it is also clear that neurons do have a strategy of making some intra-areal long range connections, and so one might expect greater variances in the ratios for higher order segments. Indeed, higher-order (>2) bifurcation and length ratios of axons do vary more than those of the lower orders (Fig. 6*C–F*). Their increased variance is partly explained on numerical grounds. The data necessarily contain a smaller number of high order segments than low ones. For example, orders 5–7 never have >7 segments for the individual axonal trees. The increased variance in the length ratio is also partly due to the inhomogeneous extension of higher order segments. It is often one or a few of these high order segments that extend much further than other segments of similar order. Usually, these long segments are formed by the vertical or horizontal running axons of spiny neurons or thalamic afferents that innervate different layers or functional columns. Basket cells can also form such segments.

If these few segments all have the same order, the result will be a large length ratio [i.e. Fig. 6*F*, p2/3:C-E, ss4(L4):B, lgnY]. However, these obviously extending segments are often of different orders. The admixture of very local smaller segments results in a smaller length ratio [i.e. Fig. 6*F*, p6(L4)]. In this sense, the large variation of length ratios of higher orders indicates that there is at least some regional specificity in the axonal tree. That is, a few collaterals will break the default axonal growth rule in the interests of extending the arbor to a more distant cortical region. However, there are clearly many ways how generation of branches can be introduced in a tree, and the question to what extent the methods of Horton and Strahler captures the true biological development of axonal trees needs further analysis.

Tree Complexity

The Strahler number (i.e. the number of times a tree can be pruned) gives an indication of the 'complexity' of axonal branching. The number can vary up or down with increasing magnitude. For example, for the herringbone tree the Strahler number is a constant 2, which is the lowest possible Strahler number of a binary tree. For the dichotomous tree the Strahler number equals the height of the tree and no other binary tree of smaller magnitude can form higher Strahler numbers. Smooth cells, which tend to have higher magnitudes (i.e. more end collaterals) than spiny cells, also tended to have a Strahler number that was 1 or 2 greater than the typical number of 5–6 for most spiny cells and thalamic afferents (Fig. 7*C*). The layer 6 pyramidal cells had the least complex branching and thus the lowest Strahler number (5).

Another more frequently applied measure of the complexity of axonal shape is the fractal dimension, which showed a weak tendency to be higher for smooth cells (Fig. 8*D*). Again, this suggests that the axons of smooth cells are slightly more complex than spiny neurons.

Growth Model

Based on topological and metrical properties of adult trees alone, it is difficult to deduce the precise growing rule that generates the tree. Nevertheless, growing rules which are not consistent with the observed parameters can be excluded. For example, the measured fractal dimension of retinal ganglion dendrites is about 1.68 (Caserta *et al.*, 1995), which is similar to the fractal dimension of a tree structure grown by diffusion limited aggregation ('DLA cluster') in two dimensions (Tolman and Meakin, 1989). This has led to the suggestion that dendrites are created by this process (Caserta *et al.*, 1990). For cortical axons, this growth process can be ruled out. The fractal dimension of the reconstructed axonal trees is always <2 (Fig. 8*D*), while three dimensional DLA clusters have a fractal dimension of ~2.5 (Tolman and Meakin, 1989).

Galton–Watson branching processes are the oldest and best understood branching processes. They appear in many variants and are applied in many sciences (Jagers, 1975), including the modeling of dendritic trees (Kliemann, 1987). We used it here in its simplest form to simulate axonal branching. Its key

properties are constant elongation, branching and stopping probabilities, and the assumption that these events are statistically independent for the end-tips of the growing tree. Despite its simplicity, the model produces trees with bifurcation ratios, length ratios and branch length distributions that are similar to the ones observed for the spiny and smooth population of the reconstructed neurons (Fig. 9*B*,*C*).

The model fails to reproduce finer details of the axonal trees, such as their lack of very small branch lengths (Fig. 9*B*,*C*). This indicates that for a better fit, the assumption of constant probabilities should be relaxed. In addition, the model simulates only the distal subtrees of the axonal trees (i.e. subtrees which have a root of order 2 or 3) and fails to predict bifurcation and length ratios of higher order (see Fig. 9*B*,*C*). The model's prediction of the second order bifurcation ratio of the subtrees of order 3 fitted worst. The reason for this failure is that the simple model does not contain a mechanism for atypical elongation of a few high-order branches ('specific' branching), as described above.

While many studies model dendritic trees, for references see Van Pelt *et al.* (2001), there is only one study that attempted to model the local branching of axonal trees (Nelken, 1992). The model used in the study of Nelken (1992) is also a Galton–Watson branching process, but slightly more complicated than our approach because it involves the distinction of several types of axonal branches. Although the model results were compared with data from axons of the somatosensory cortex of the mouse, the comparison was qualitative and no details about the fitted model parameters were given.

Conclusion

At face value, the structure of the axons of various types of cortical neurons seems to be distinctly different from one another. However, the topological structure of axons is not easily detected by simple observation. Therefore, we have applied a battery of analyses that are sensitive to the topological characteristics of the reconstructed axonal trees.

Surprisingly, our results revealed no dramatic differences in the fundamental organization of the axonal arbors of neurons as distinct as basket cells and pyramidal cells, except for their scales of collateral length. Instead, we found a marked topological resemblance between the trees of all axons, suggesting that they all grow according to the same basic rules. We have demonstrated that even a simple three-parameter axonal growth model can generate trees with characteristics that are nearly indistinguishable from those of intra-areal cortical axons.

Obviously there are many other branching processes that might also produce the observed length ratios, bifurcation ratios and branch length distributions of the distal subtrees of the measured axons. Much more analysis is needed to specify more completely the branching process of axonal trees. In particular, a simple mechanism for the atypical collateral extension that seems to support clustering of the tree branches in 3D space, would be a useful next step.

Although we now can describe the generic structure of axons, the particular instantiation of an axon in 3D space is another matter. Presumably, the 3D space instantiation will take the topological rules as growth constraints, and configure themselves to satisfy connection constraints, which have not been addressed here.

That even our simple model reproduces the observed values raises the possibility that only a minimal set of specific rules is actually used when the axon of any type of cortical neuron grows and branches to form connections with other neurons. Small parametric adjustments in the rules could be sufficient to explain the different macroscopic structures of axons that are (superficially) characteristic of different neuronal types. In this context it is interesting to note that a simple generation rule was also found for the placement of boutons along the branches of cortical axons (Braitenberg and Schüz, 1991; Anderson *et al.*, 2002). These simplifications have interesting implications for models of the development of complex neuronal networks such as cortex.

Notes

This work was supported by EU grant (QULG3-1999-01064) and HFSP grant (RG0123/2000-*B*) to K.M.

Address correspondence to Tom Binzegger, School of Biology, Henry Wellcome Building for Neuroecology, University of Newcastle upon Tyne NE2 4HH, UK. Email: tom.binzegger@ncl.ac.uk.

References

Anderson JC, Binzegger T, Douglas RJ, Martin KAC (2002) Chance or design? Some specific considerations concerning synaptic boutons in cat visual cortex. J Neurocytol 31:211–229.

Bart AG, Kozhanov VM, Chmykhova NM, Botchkina NA, Ternovaya LA, Clamann GP (2000) Topological and statistical analysis of 3-D reconstructions of axon collaterals. Neurophysiology 32:249–259.

Braitenberg V, Schüz A (1991) Anatomy of the cortex. Berlin: Springer.

Caserta F, Stanley HE, Eldred WD, Daccord G, Hausman RE, Nittmann J (1990) Physical mechanism underlying neurite outgrowth: a quantitative analysis of neuronal shape. Phys Rev Letters 64:95–98.

Caserta F, Eldred WD, Fernández E, Hausman RE, Stanford LR, Bulderev SV, Schwarzer S, Stanley HE (1995) Determination of fractal dimension of physiologically characterized neurons in two and three dimensions. J Neurosci Meth 56:133–144.

Changizi MA (2001) Principles underlying mammalian neocortical scaling. Biol Cybern 84:207–215.

Douglas RJ, Martin KAC, Whitteridge D (1991) An intracellular analysis of the visual responses of neurons in cat visual cortex. J Physiol Lond 440:659–696.

Fernández E, Jelinek HF (2001) Use of fractal theory in neuroscience: methods, advantages, and potential problems. Methods 24:309–321.

Foh E, Haug H, König M, Rast A (1973) Quantitative Bestimmung zum feineren Aufbau der Sehrinde der Katze, zugleich ein methodischer Beitrag zur Messung des Neuropils. Microsc Acta 75:148–168.

Friedlander MJ, Stanford LR (1984) Effects of monocular deprivation on the distribution of cell types in the LGN_d: a sampling study with fine-tipped micropipettes. Exp Brain Res 53:451–461.

Gupta A, Wang Y, Markram H (2000) Organization principles for a diversity of GABAergic interneurons and synapses in the neocortex. Science 287:273–278.

Innocenti GM, Lehmann P, Houzel JC (1994) Computational structure of visual callosal axons. Eur J Neurosci 6:918–935.

Jagers P (1975) Branching processes with biological applications. London: John Wiley.

Jones EG (1975) Varieties and distribution of non-pyramidal cells in the somatic sensory cortex of the squirrel monkey. J Comp Neurol 160:205–268.

Kisvárday ZF, Martin KAC, Whitteridge D, Somogyi P (1985) Synaptic connections of intracellularly filled clutch neurons: a type of small basket neuron in the visual cortex of the cat. J Comp Neurol 241:111–137.

Kisvárday ZF, Martin KAC, Freund TF, Maglóczky ZS, Whitteridge D, Somogyi P (1986) Synaptic targets of HRP-filled layer III pyramidal cells in the cat striate cortex. Exp Brain Res 64:541–552.

Kliemann W (1987) A stochastic dynamical model for the characterization of the geometrical structure of dendritic processes. Bull Math Biol 49:135–152.

Koulakov AA, Chklovskii DB (2001) Orientation preference patterns in mammalian visual cortex: a wire length minimization approach. Neuron 29:519–527.

Lorente de Nó R (1949) Cerebral cortex: architecture, intracortical connections, motor projections. In: Physiology of the nervous system (Fulton J, ed.), pp. 288–313. New York: Oxford University Press.

Lund JS, Boothe RG (1975) Interlaminar connections and pyramidal neuron organisation in the visual cortex, area 17, of the macaque monkey. J Comp Neurol 159:305–334.

Lund JS, Henry GH, MacQueen CL, Harvey AR (1979) Anatomical organization of the primary visual cortex (area 17) of the cat. A comparison with area 17 of the macaque monkey. J Comp Neurol 184:599–618.

MacDonald N (1983) Trees and networks in biological models. New York: John Wiley.

Mandelbrot BB (1983) The fractal geometry of nature. New York: Freeman.

Martin KAC, Whitteridge D (1984) Form, function and intracortical projections of neurones in the striate visual cortex of the cat. J Physiol Lond 353:463–504.

Mitchison G, Crick F (1982) Long axons within striate cortex: their distribution, orientation and patterns of connections. Proc Natl Acad Sci USA 79:3661–3665.

Nelken I (1992) A probabilistic approach to the analysis of propagation delays in large cortical axonal trees. In: Information processing in the cortex: experiments and theory (Aertsen A, Braitenberg V, eds), pp. 29–49. Berlin: Springer.

Pelt JV, Uylings HB, Verwer RW, Pentney RJ, Woldenberg MJ (1992) Tree asymmetry — a sensitive and practical measure for binary topological trees. Bull Math Biol 54:759–784.

Ramón y Cajal S (1908) Histologie du système nerveux. Madrid: CSIC (reprinted 1972).

Rockland KS (1995) Morphology of individual axons projecting from area V2 to MT in the macaque. J Comp Neurol 355:15–26.

Strahler AN (1952) Hypsometric (area-altitude) analysis of erosional topology. Bull Geol Soc Am 63:1117–1142.

Szentagothai J (1975) The 'module-concept' in cerebral cortex architecture. Brain Res 95:475–496.

Tarboton DG, Bras RL, Rodriguez-Iturbe I (1988) The fractal nature of river networks. Water Resour Res 24:1317–1322.

Tettoni L, Gheorghita-Baechler F, Bressoud R, Welker E, Innocenti GM (1998) Constant and variable aspects of axonal phenotype in cerebral cortex. Cereb Cortex 8:543–552.

Tolman S, Meakin P (1989) Off-lattice and hypercube-lattice models for diffusion-limited aggregation in dimensionalities 2–8. Phys Rev A 40:428–437.

Triller A, Korn H (1986) Variability of axonal arborizations hides simple rules of construction: a topological study from HRP intracellular injections. J Comp Neurol 253:500–513.

Uylings HBM, Van Pelt J (2002) Measures for quantifying dendritic arborizations. Network 13:397–414.

Van Pelt J, van Ooyen A, Uylings HBM (2001) The need for integrating neuronal morphology databases and computational environments in exploring neuronal structure and function. Anat Embryol 204: 255–265.